

Article

Characterization of Shallow Groundwater Circulation Based on Chemical Kinetics: A Case Study of Xiong'an New Area, China

Yubo Xia ^{1,2,*}, Haitao Li ³, Bing Wang ⁴, Zhen Ma ^{1,2}, Xu Guo ^{1,2}, Kai Zhao ³ and Changrong Zhao ^{1,2}

¹ Tianjin Center China Geological Survey (CGS), Tianjin 300170, China; tjmazhen@126.com (Z.M.); telent12@163.com (X.G.); tjzchangrong@163.com (C.Z.)

² North China Center for Geoscience Innovation, Tianjin 300170, China

³ China Institute of Geo-Environment Monitoring, Beijing 100081, China; lihaitao@mail.cgs.gov.cn (H.L.); zhaokai1987924@163.com (K.Z.)

⁴ Tianjin Geothermal Exploration and Development-Designing Institute, Tianjin 300250, China; wangbingdry@126.com

* Correspondence: sosodragon@163.com; Tel.: +86-022-8411-2916

Abstract: Xiong'an New Area, located in the middle of the North China Plain, will have been built as a "city of the future." Urban planning and construction need to comprehensively consider the constraints of hydrogeological conditions such as aquifer structure and parameters. As the main aquifer in this area, the paleo-channel is heterogeneous and anisotropic, and the two-dimensional hydraulic conductivity in each horizontal direction cannot be obtained from aquifer tests. Therefore, this study adopts a chemical kinetics method to calculate the ionic activity and mineral saturation indices of shallow groundwater, determine the groundwater chemical potential field, and construct a horizontal two-dimensional groundwater chemical kinetics model. This model is used to calculate the hydraulic conductivity, flow rate and retention time of groundwater in areas of different chemical kinetics, as well as evaluate horizontal heterogeneity of the Quaternary paleo-channel aquifer. The results indicate that the groundwater chemical potential field can reflect the characteristics of the groundwater seepage field in each horizontal direction. The paleo-channel is the main channel of groundwater circulation, which shows the statistical difference of its permeability. Alluvial and lacustrine strata affect groundwater circulation due to their different hydrogeological structures and permeability. The groundwater chemical kinetics results of hydraulic conductivity along the paleo-channel are approximately consistent with traditional hydrogeological calculation results derived from aquifer test data. Hydraulic conductivity is higher in the extension direction of the paleo-channel, and lower if the path crosscuts multiple paleo-channels. This feature can be used to build a hydrogeological structure model combined with drilling data. Furthermore, excessive groundwater exploitation will change the actual flow rate and retention time of groundwater, thereby affecting the groundwater circulation conditions. This study of groundwater circulation in Xiong'an New Area by means of chemical kinetics makes up for the deficiency in the study of the unconsolidated sedimentary aquifer anisotropy within the paleo-channel.

Keywords: chemical kinetics; mineral saturation index; hydraulic conductivity; heterogeneity; Xiong'an New Area



Citation: Xia, Y.; Li, H.; Wang, B.; Ma, Z.; Guo, X.; Zhao, K.; Zhao, C.

Characterization of Shallow Groundwater Circulation Based on Chemical Kinetics: A Case Study of Xiong'an New Area, China. *Water* **2022**, *14*, 1880. <https://doi.org/10.3390/w14121880>

Academic Editors: Zhonghe Pang, Fengtian Yang and Pingheng Yang

Received: 25 April 2022

Accepted: 7 June 2022

Published: 11 June 2022

Publisher's Note: MDPI stays neutral with regard to jurisdictional claims in published maps and institutional affiliations.



Copyright: © 2022 by the authors. Licensee MDPI, Basel, Switzerland. This article is an open access article distributed under the terms and conditions of the Creative Commons Attribution (CC BY) license (<https://creativecommons.org/licenses/by/4.0/>).

1. Introduction

Groundwater is a crucial resource for various socio-economic activities [1]. Groundwater contains many dissolved inorganics with a wide variety of chemical constituents, whose concentrations depend on interactions between the water and water-bearing sediments [2]. As groundwater passes through different geological units, the concentration of dissolved substances typically increases [3]. The water cycle not only comprises different water parts,

but is also a geochemical process involving mineral dissolution/precipitation, ion oxidation/reduction, and ion exchanges [4]. During this process, groundwater components migrate, accumulate and divide along the groundwater flow path [5]. As such, the natural composition of water molecules, hydrogen and oxygen isotopes mark the water cycle process and play an indicator role in the study of groundwater interactions [6]. The degree of hydrochemical evolution is largely determined by the residence time of the water within the aquifer, i.e., by the duration of the water–rock interaction [7]. Hydrogeochemical tools can clearly differentiate different water types originating from mountain front recharge, artesian discharge, river leakage or floodwater recharge [8]. By analyzing the historical database of groundwater major ion chemistry, the connectivity between alluvium aquifer and basin can be investigated [9,10]. Therefore, understanding the different processes controlling groundwater quality is crucial for groundwater circulation.

Xiong'an New Area is located in the Baiyangdian Lake basin, in Hebei Province, North China, with Baiyangdian Lake forming the final confluence point within the region (Figure 1). Nine rivers flow into the lake; however, the only discharge path is the Zhaowangxin River from the east side. Highly developed agriculture, a high degree of groundwater exploitation and intense artificial irrigation in this region have continuously reduced the amount of groundwater resources in the North China Plain [11], with farmland irrigation in Hebei Province accounting for approximately 85% of all groundwater exploitation [12]. Groundwater quality is affected by many aspects of the existing groundwater environment [13]. For shallow groundwater, the quality is not only controlled by both surface water and groundwater, but also by sedimentary conditions since the Quaternary [14]. Xiong'an New Area is selected as the study area because it is located in an alluvial-proluvial plain, and the aquifer is mainly developed in the form of a paleo-channel (Figure 2), which is heterogeneous and anisotropic [15]. The groundwater chemical dynamics method can therefore be utilized to full advantage in providing a two-dimensional calculation to solve the key problems in groundwater circulation and provide hydrogeological parameters for the planning and construction of Xiong'an New Area.

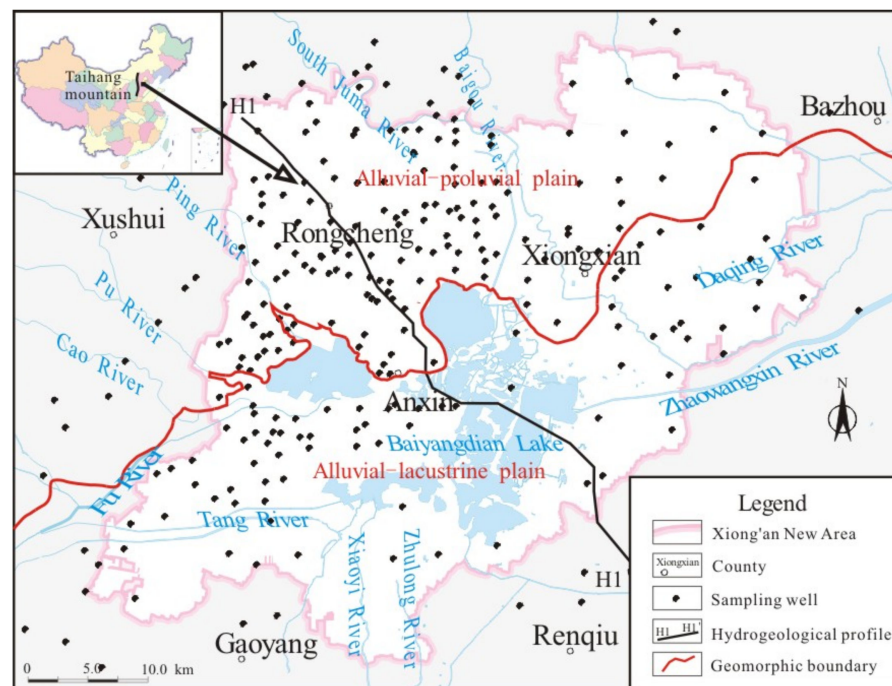


Figure 1. Location of sampling points and the hydrogeological profile in the study area.

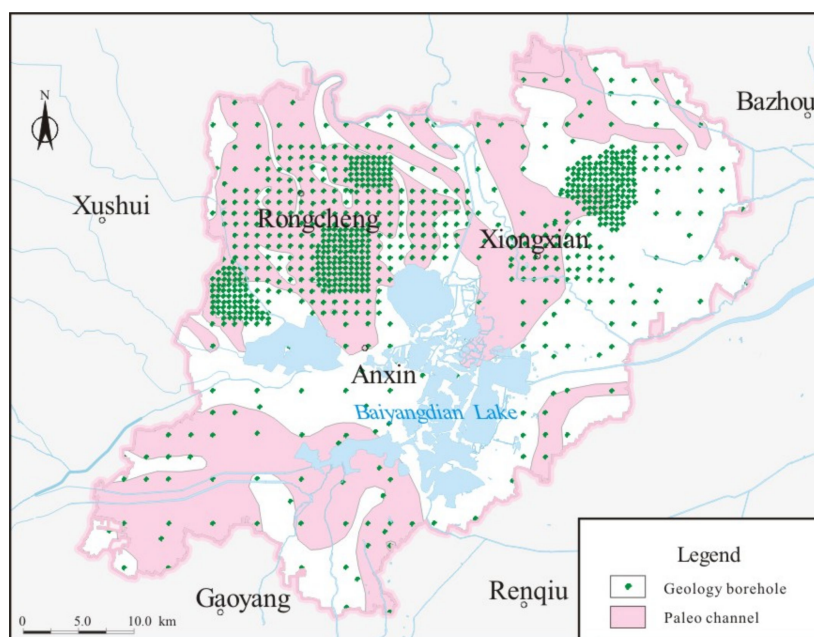


Figure 2. Pleistocene paleo-channel distribution map inferred by boreholes.

In comparison to traditional hydrogeological research (e.g., field aquifer tests), groundwater chemical kinetics research employs the hydrogeological unit to determine spatiotemporal changes in the water flow field and water quality concentration field, whose kinetic parameters are a function of space and time [5]. By analyzing the formation of groundwater kinetic and hydrochemical fields, dynamics of groundwater and chemical kinetics can be coupled to evaluate groundwater quantity, surface water quality and water environments to more effectively solve practical problems related to water resources and the ecological environment [16]. This method has been widely used in the study of groundwater circulation in karstic spring basins [17–19]. In karst aquifer system, the geological structure controls the flow direction of groundwater [20,21]. The lithology is mainly limestone, meaning that the chemical components of groundwater are high in these subregions. Carrying out groundwater chemical kinetics evaluation along the direction of groundwater flow allows for the calculation of the relevant parameters and can assist in restoring the groundwater circulation conditions. In the unconsolidated sedimentary pore aquifer, especially in the Quaternary sedimentary layers with complex hydrogeological conditions and intricate paleo-channels, the material source of groundwater and flow conditions are uneven, due to the diversity of minerals in the stratum and the heterogeneity of the hydrogeological structures [22,23], and so groundwater chemical kinetics has not been widely used in such contexts. Taking Xiong'an New Area as an example, using the data of 283 wells, a Middle Pleistocene paleo-channel map of the main aquifers can be reconstructed. Comprehensive interpretation of local high-density borehole and geomorphic data can determine the distribution of some paleo-channels, and then determine the structure of the aquifers. The pattern of the Middle Pleistocene aquifer is then verified by calculating the connectivity between paleo-channels. Based on the results of groundwater chemical dynamics, the distribution of paleo-channels in areas with low borehole density can be inferred. The groundwater circulation in the alluvial-proluvial and alluvial-lacustrine plains can therefore be studied, which makes up for the lack of research on unconsolidated sedimentary aquifers in which paleo-channels are the main aquifers.

The purpose of this study is to establish a chemical kinetic model of the groundwater in Xiong'an New Area. This model is then used as follows: (1) to calculate the hydrogeological parameters in the direction of the flow field; (2) to analyze the shallow groundwater circulation conditions according to the principles of groundwater chemical kinetics; and

(3) to analyze the applicability of groundwater chemical kinetics to studying unconsolidated sedimentary aquifers with paleo-channels as the main aquifers.

2. Materials and Methods

2.1. Study Area

The study area is Xiong'an New Area, Hebei Province, China, which is a sedimentary plain landform located in front of an alluvial plain in the eastern foothills of Taihang mountain. The elevation of the terrain gradually decreases from northwest to southeast and ranges from 5 m to 26 m amsl, with slopes of less than 2‰. The region, which has an area of 1800 km² (within the pink boundary range in Figure 1), can be further divided into an alluvial-proluvial plain and an alluvial-lacustrine plain (red boundary in Figure 1), according to its different landforms.

An alluvial-proluvial plain subregion is located in the north of Xiong'an New Area, which lies mainly to the north of the border between Xiongqian County and Rongcheng County. The upper part comprises a modern river alluvium or fan-delta-front depression deposits, with an underlying alluvial-diluvial layer. The alluvial-lacustrine plain subregion is located in the south-central part of the study area, to the south of the border between Xiongqian County and Rongcheng County. It comprises a modern river alluvium and lake and marsh deposits [24]. The surface outcrop layer in Xiong'an New Area is an unconsolidated Quaternary layer. According to preliminary survey results, the thickness of the Quaternary sediments in the study area is generally 135 m [25], and the genetic types are predominantly alluvial, proluvial and lacustrine. The Quaternary aquifer is the research object of this study.

The unconsolidated sedimentary aquifer of the North China Plain can be divided into four aquifer groups, according to the general division method [26]. The first and second aquifer groups are shallow groundwater, the layer that is most exploited, and their genetic age is Quaternary; the third and fourth aquifer groups are deep groundwater, and their genetic age is Tertiary. The first aquifer group is phreatic water and is partially over exploited, with a bottom depth in the study area of generally less than 10 m, and its genetic age is Holocene. The second aquifer group has an average bottom depth of 120 m, and its genetic age is Pleistocene. The second aquifer group is over exploited, which means the water head is not 3 m higher than the aquifer. The shallow groundwater consists of multiple locally continuous aquifers and exists in the form of paleo-channels. The lithology of the aquifers is mainly fine and silty sand, with local medium and coarse sand. The aquifer groups are separated by relatively continuous aquicludes and controlled by sedimentary structures.

The shallow groundwater in the study area is predominantly recharged by precipitation, agricultural irrigation, surface water infiltration and lateral flow, and predominantly discharged by artificial mining, groundwater flow and evaporation. Under current conditions, the shallow groundwater flows from northwest to southeast. Due to the low exploitation intensity of groundwater, a local water mound formed near Baiyangdian Lake (Figure 3). Research involving hydrogen and oxygen isotopes in Baiyangdian basin has shown that the groundwater in Baiyangdian and its surrounding areas is supplied by atmospheric precipitation and lake water at the same time. The impact range of lake water leakage on groundwater is mainly concentrated in the upper layer, and the vertical impact depth is about 20 m [27,28]. The relatively high water level in Baiyangdian is mainly due to lower groundwater exploitation. The specific capacity of the shallow groundwater is 1000–3000 m³/d, which represents moderate enrichment. In the northwest of Anxin County, the southwest of Rongcheng County and the east of Xiongqian County, the specific capacity is 300–1000 m³/d, which denotes weak enrichment. The depth of the shallow groundwater level is typically 5–20 m, and the depth of groundwater in the area surrounding Baiyangdian Lake is relatively shallow, at less than 5 m.

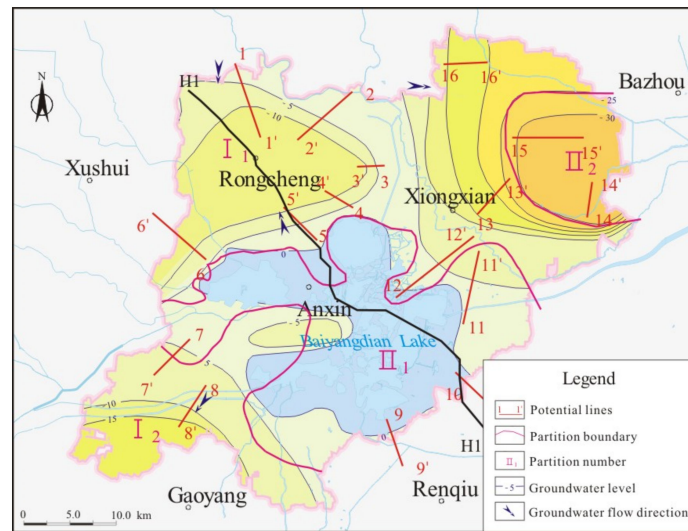


Figure 3. Potential lines of shallow water and subzones of the study area divided according to the groundwater chemical kinetics.

Hydrochemical types are evaluated according to the Shchukarev classification. According to the spatial distribution of main ions, the main chemical characteristics of sampled groundwater and the mineral composition and particle size of sediments in contact with water, three hydrochemical areas are determined in Figure 4. These are as follows: Zone A: the areas far away from Baiyangdian are mainly affected by upstream water, and the hydrochemical types are mainly $\text{HCO}_3\text{-Ca}$ and $\text{HCO}_3\text{-Ca-Mg}$; Zone C: Located in Baiyangdian and the east of Xiongqian, with hydrochemical types that are affected by lacustrine sedimentary strata and mainly comprise $\text{SO}_4\text{-HCO}_3\text{-Na-Mg}$; Zone B: This is a transition zone, and the hydrochemical types are $\text{HCO}_3\text{-SO}_4\text{-Na-Mg-Ca}$, $\text{HCO}_3\text{-Cl-Na-Ca-Mg}$ and $\text{HCO}_3\text{-SO}_4\text{-Cl-Na-Mg}$.

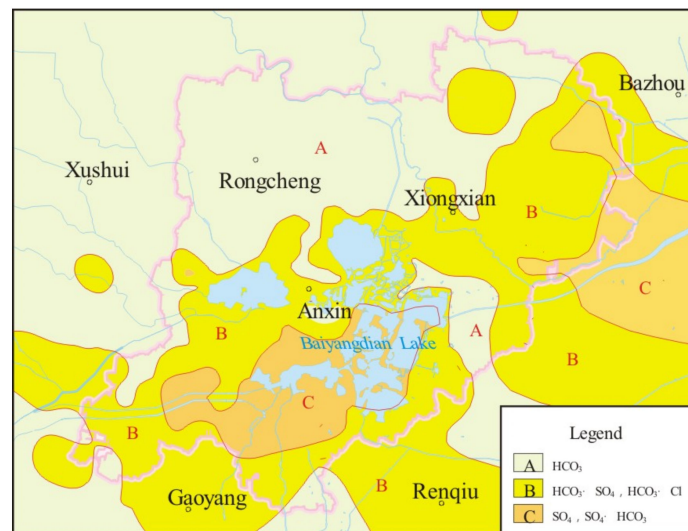


Figure 4. Hydrochemical types of shallow groundwater in Xiong’an New Area.

2.2. Experimental Methods

The hydrogeological profile used in this study is shown in Figure 5, and its map location is shown in Figure 1. In June 2017, water samples for chemical analysis were obtained from 283 wells with a depth of 50–140 m. The groundwater level, measured at the same time, was used to draw a shallow groundwater level map (Figure 3). Aquifer tests were carried out in 12 boreholes of four subzones, and the aquifer hydraulic conductivity

was calculated according to the unsteady flow method. In the field, a HACH SL1000 Portable Parallel Analyzer was used to measure the conductivity, pH, air temperature, water temperature, alkalinity, hardness and dissolved oxygen content of groundwater in the wells. The alkalinity and carbon dioxide content were determined by titration.

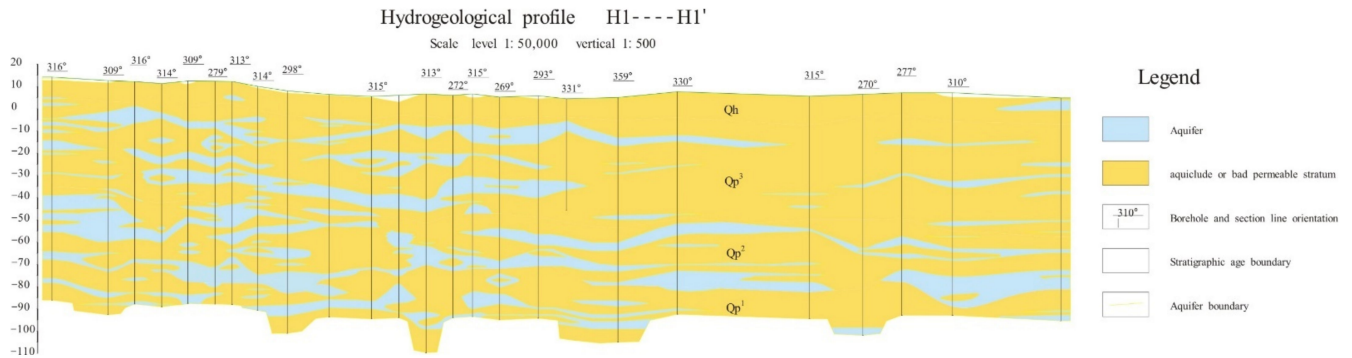


Figure 5. Hydrogeological profile in Xiong’an New Area H1——H1’.

The main ions (Na^+ , K^+ , Ca^{2+} , Mg^{2+} , SO_4^{2-} and Cl^-) in the samples were analyzed in the laboratory. Measurements were made within 48 h of collection. Titration was used to determine the calcium, magnesium, chloride and dissolved oxygen contents. Sodium and potassium contents were determined by flame photometry and sulfate content was determined by the spectrophotometric turbidimetric method. These test methods were conducted according to the Chinese specifications. The test amounts of parallel samples was not less than 10%, and the results were compared with the blank samples. The test results met the requirements of quality specifications.

2.3. Relationship between Ionic Activity and Concentration in Groundwater

Ion activity in water is reduced by ionic electrostatic attraction, which restricts the chemical action of ions, and this trend in groundwater with high salinity is relatively obvious. In order to ensure that ion reactions are accurately expressed, the ion concentration (C_i , $\text{mmol}\cdot\text{L}^{-1}$) obtained from water analysis should be modified to obtain the ionic activity (α_i , $\text{mmol}\cdot\text{L}^{-1}$).

The relationship between α_i and C_i is:

$$\alpha_i = f_i C_i \tag{1}$$

where f_i (dimension, 1) is the activity coefficient. Activity is related to the ionic force (I , $\text{mol}\cdot\text{L}^{-1}$), which can be converted through Equation (2):

$$I = \frac{1}{2} \sum C_i Z_i^2 \tag{2}$$

where C_i is the concentration of i ions in a solution and Z_i is the electricity valence of the ions. When the groundwater is fresh water, I is typically less than 0.1, and the Debye–Huckel formula can be used:

$$\lg f_i = - \frac{AZ^2\sqrt{I}}{1 + Ba_i^2\sqrt{I}} \tag{3}$$

Here, a_i (nm) is the effective diameter of ion i and A and B are constants expressing solvent characteristics under a specific temperature and pressure, which change with temperature. The regression equation is as follows:

$$\begin{aligned} A &= 0.485 + 0.00092T \\ B &= 0.3241 + 0.000162T \end{aligned} \tag{4}$$

where T is the water temperature ($^{\circ}\text{C}$), which is $0\text{--}60$ $^{\circ}\text{C}$ for the above formula. When the groundwater is not fresh water, $I \geq 0.1$ and the Davis equation can be used:

$$\lg f_i = -0.505 Z_i^2 \left(\frac{\sqrt{I}}{1 + \sqrt{I}} - 0.2I \right) \quad (5)$$

2.4. Calculation of the Mineral Saturation Index in Groundwater

The activity and concentration of component i at any point in the hydrochemical field can be expressed by α_i and C_i . Groundwater cannot continuously dissolve mineral j and accommodate component i from other minerals; this process is controlled by the solubility product law of mineral j . The representative mineral j restricts saturation index β_j of the direction of dissolution and precipitation, the extent of the reaction and the changes in hydrochemical type. A change of the hydrochemical potential field can be represented by the activity gradient $\Delta\alpha_{ij}$. Moreover, the values of α_i and β_i can be calculated by means of chemical thermokinetics [29]. The saturation indices for several common minerals are as follows:

Saturation index of calcite:

$$\beta_c = \frac{K_2 \times \alpha_{\text{Ca}^{2+}} \times \alpha_{\text{HCO}_3^-}}{K_c \times \alpha_{\text{H}^+}} \quad (6)$$

Saturation index of dolomite:

$$\beta_d = \frac{\alpha_{\text{Ca}^{2+}} \times \alpha_{\text{Mg}^{2+}} \times K_2^2 \times \alpha_{\text{HCO}_3^-}^2}{K_d \times \alpha_{\text{H}^+}^2} \quad (7)$$

Saturation index of gypsum:

$$\beta_g = \frac{\alpha_{\text{Ca}^{2+}} \times \alpha_{\text{SO}_4^{2-}}}{K_g} \quad (8)$$

Saturation index of halite:

$$\beta_h = \frac{\alpha_{\text{Na}^+} \times \alpha_{\text{Cl}^-}}{K_h} \quad (9)$$

where K_2 is the second order dissociation constant of carbonic acid; K_c is the dissociation constant of calcite; K_d is the dissociation constant of dolomite; K_g is the dissociation constant of gypsum; and K_h is the dissociation constant of halite.

The equilibrium constant of the chemical reaction varies with temperature, and can be obtained experimentally or derived from thermochemical data using the quadratic interpolation polynomial of $\text{p}K_j$ ($-\lg K$) through the regression of temperature:

$$\text{p}K_{(t)} = a + 10^{-4}b(T - T_t) + 10^{-6}c(T - T_t)^2 \quad (10)$$

where a , b and c are polynomial coefficients obtained by regression; T is the temperature ($^{\circ}\text{C}$) of the water sample; and T_t is the experimental temperature ($^{\circ}\text{C}$).

The temperature correction constants for different mineral are given below:

Dissociation constant of calcite:

$$\text{p}K_c = 8.34 + 123.33 \times 10^{-4}(T - 25) + 22.22 \times 10^{-6}(T - 25)^2 \quad (11)$$

Dissociation constant of dolomite:

$$\text{p}K_d = 16.29 + 185 \times 10^{-4}(T - 15) + 250 \times 10^{-6}(T - 15)^2 \quad (12)$$

Dissociation constant of gypsum:

$$pK_g = 4.61 - 7 \times 10^{-4}(T - 25) + 75.33 \times 10^{-6}(T - 25)^2 \quad (13)$$

First order dissociation of each mineral:

$$pK_1 = 6.35 - 52.5 \times 10^{-4}(T - 25) + 175 \times 10^{-6}(T - 25)^2 \quad (14)$$

Secondary order dissociation of each mineral:

$$pK_2 = 10.33 - 90 \times 10^{-4}(T - 25) + 111.11 \times 10^{-6}(T - 25)^2 \quad (15)$$

Henry constant:

$$pK_H = 1.47 - 123 \times 10^{-4}(T - 25) + 66.7 \times 10^{-6}(T - 25)^2 \quad (16)$$

The groundwater chemical kinetic constant k_j ($\times 10^{-8} \text{ mol}\cdot\text{L}^{-1}\cdot\text{d}^{-1}$) can be obtained by sample testing and field testing, using the following equations:

Chemical kinetic constant of calcite:

$$k_c = \frac{2\bar{K}\Delta h \left(\Delta a_{\text{Ca}^{2+}} - \Delta a_{\text{Mg}^{2+}} - \Delta a_{\text{SO}_4^{2-}} \right)}{\Delta S^2(2 - \beta_{cA} - \beta_{cB})} \quad (17)$$

$[\Delta a_{\text{Ca}^{2+}} > \Delta a_{\text{Mg}^{2+}} + \Delta a_{\text{SO}_4^{2-}}; 2 > \beta_{cA} + \beta_{cB}]$

Chemical kinetic constant of dolomite:

$$k_d = \frac{2\bar{K}\Delta h \Delta a_{\text{Mg}^{2+}}}{\Delta S^2(2 - \beta_{dA} - \beta_{dB})} \quad (18)$$

$[\Delta a_{\text{Mg}^{2+}B} \geq \Delta a_{\text{Mg}^{2+}A}; 2 > \beta_{dA} + \beta_{dB}]$

Chemical kinetic constant of gypsum:

$$k_g = \frac{2\bar{K}\Delta h \Delta a_{\text{SO}_4^{2-}}}{\Delta S^2(2 - \beta_{gA} - \beta_{gB})} \quad (19)$$

$[\Delta a_{\text{SO}_4^{2-}B} \geq \Delta a_{\text{SO}_4^{2-}A}; 2 > \beta_{gA} + \beta_{gB}]$

Chemical kinetic constant of halite:

$$k_h = \frac{2\bar{K}\Delta h \Delta a_{\text{Cl}^-}}{\Delta S^2(2 - \beta_{hA} - \beta_{hB})} \quad (20)$$

$[\Delta a_{\text{Cl}^-B} \geq \Delta a_{\text{Cl}^-A}; 2 > \beta_{hA} + \beta_{hB}]$

2.5. Calculation of Groundwater Parameters

Since the basic minerals constituting all carbonates and sulfates are calcite, dolomite, gypsum and halite, the theory of simultaneous dissolution and separate precipitation of multiple minerals is needed in the study of hydrogeochemical field [5,29]. The groundwater hydraulic conductivity, retention time and velocity were calculated for the study area [5]. The formula for the groundwater hydraulic conductivity can be derived from Darcy's law:

$$K_{iAB} = \frac{\Delta S_{AB}^2 \sum_{j=1}^m v_{ij} k_j (2 - \beta_{jA} - \beta_{jB})}{2\Delta \alpha_{ijAB} \Delta h_{AB}} \quad (21)$$

where K_{iAB} (m/d) is the hydraulic conductivity determined by the chemical index of component i at any two points, A and B , on the Potential lines; Δh_{AB} is the differential water head between A points (m) and B (m); $\Delta \alpha_{ijAB}$ is the activity difference of i ions at points A and B ; β_{jA} and β_{jB} are the saturation indices of mineral j at points A and B ; ΔS_{AB} (m)

is the distance between A and B ; v_{ij} is the stoichiometric coefficient; and k_j is a chemical kinetic constant.

The groundwater retention time t (a) was calculated as follows:

$$t_{ijAB} = \frac{2n\Delta a_{ijAB}}{\sum_{j=1}^m v_{ij} \bar{k}_j (2 - \beta_{jA} - \beta_{jB})} \quad (22)$$

$$t = \frac{\Delta S_{iAB} \cdot n}{V_{niAB}} \quad (23)$$

where t_{ijAB} refers to the groundwater age of any two points, A and B , on the Potential lines showed by mineral j with i components (a); n is the porosity of the rock ($\bar{k}_j = nk_j$); and V_{niAB} is the “tracer” infiltration velocity of component i on the groundwater flow line between A and B .

The actual groundwater velocity (U m/d) was calculated as follows:

$$U_{ijAB} = \frac{V_{ijAB}}{n} = \frac{\Delta S_{iAB} \sum_{j=1}^m v_{ij} k_j (2 - \beta_{jA} - \beta_{jB})}{2n\Delta a_{ijAB}} \quad (24)$$

3. Results

3.1. Major Mineral Saturation Indices

The mineral saturation indices of groundwater can indicate the dissolved/diluted state of major ions in the minerals [30,31]. Laboratory experiments have shown that the pH value and temperature have certain effects on mineral dissolution and precipitation [32,33]. As a hydrogeological unit of alluvial-pluvial and alluvial-lacustrine, the structure of the study area is complex and diverse, and the saturation indices are influenced by the groundwater temperature [34]. In this study, the saturation index of each mineral is derived, where $\beta \geq 1$ indicates a diluted state as the basic theoretical condition for the study [35].

β_c is less than 1 around Baiyangdian Lake, Zhaowangxin River and the eastern part of Xiong'an New Area, indicating a continuous and zonal subregion, and less than zero in Rongcheng County, indicating a scattered and discontinuous subregion. β_d is greater than two around Baiyangdian Lake and in the eastern areas of Xiong'an New Area, greater than three in the southern part of Baiyangdian Lake, less than one in the eastern part of Rongcheng County and Xiongxin County, and less than zero in scattered areas of Rongcheng County, indicating a scattered distribution. The saturation indices of β_g and β_h are less than zero throughout the study area. Saturation trends are similar for β_c and β_d , with relatively high index values to the south of Baiyangdian Lake.

The isoline maps showing $\alpha_{Ca^{2+}}$ and β_c (Figure 6a; the different hydrochemical zones are shown in Figure 3) indicate an increasing trend from north to south in zone I₁ and west to east in zone I₂, and $\alpha_{Ca^{2+}}$ is generally less than 2 mmol/L. The concentration is the highest in the south of Baiyangdian Lake and northeast of Xiong'an New Area, where $\alpha_{Ca^{2+}}$ is generally greater than 2 mmol/L; $\alpha_{Ca^{2+}}$ then decreases toward the surrounding area. β_c also exhibits a consistent value that varies by less than one. β_c is less than one in most of zone I and ranges between 1 and 1.8 in zone II. Compared with the groundwater level, $\alpha_{Ca^{2+}}$ and β_c gradually increase along the groundwater flow direction. Zone I is distributed in neither a lake nor groundwater funnel area. Although there are groundwater funnels in Rongcheng, Gaoyang and other areas, the current hydrochemical field indicates no substantial hydrochemical change in the historical flow field. However, in the funnel area of the eastern part of Xiongxin County (east part of zone II), the ionic concentration and $\alpha_{Ca^{2+}}$ are higher in the funnel area (which exhibits a decrease in the water level) than in the non-funnel area, with the latter reaching a maximum value in the center of the funnel.

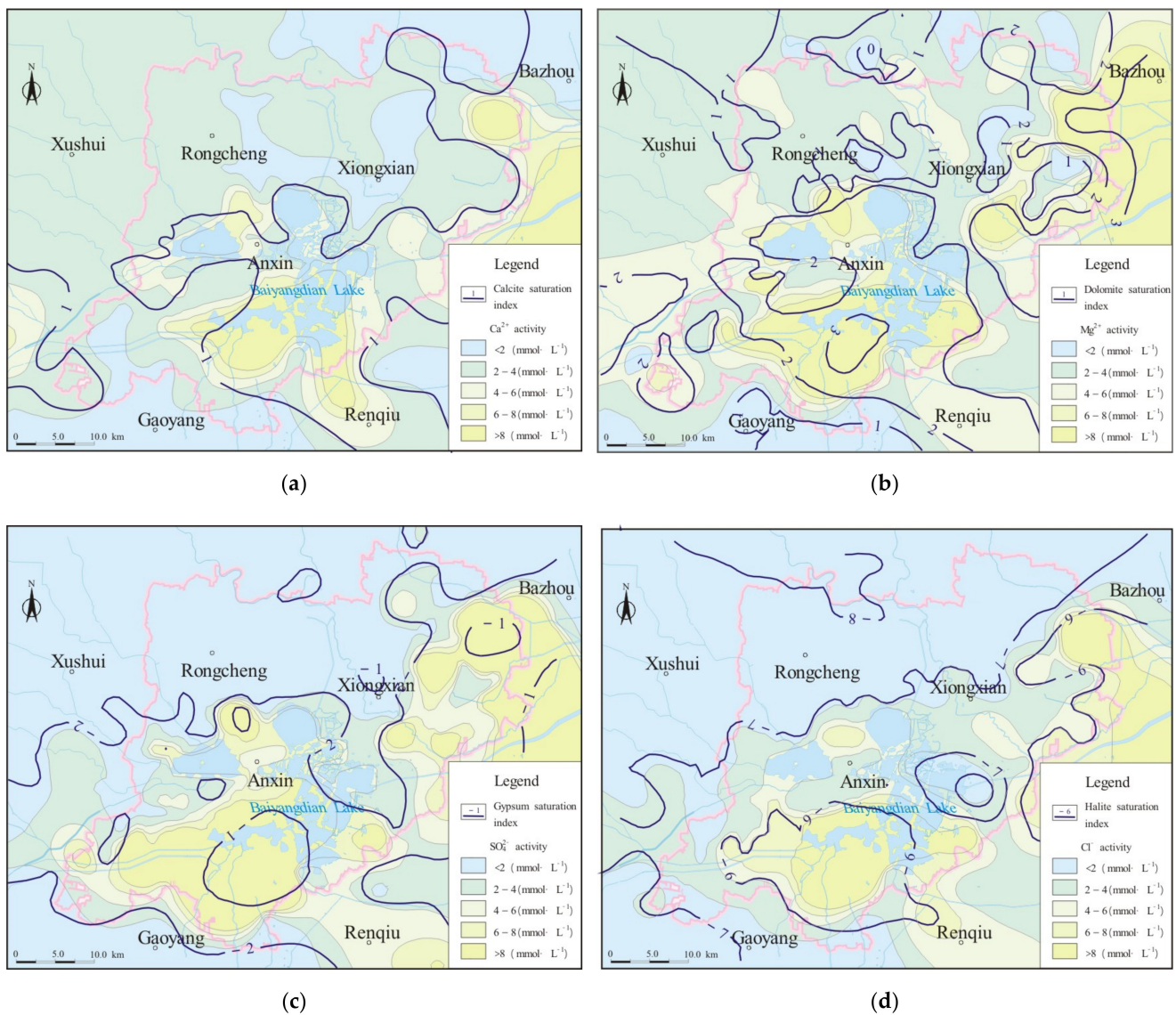


Figure 6. Isoline maps of ionic activity and mineral saturation indices (black dotted lines) for (a) calcium (Ca^{2+}) and calcite, (b) magnesium (Mg^{2+}) and dolomite, (c) sulfate (SO_4^{2-}) and gypsum and (d) chloride (Cl^-) activity and halite.

According to the isoline maps showing $\alpha_{\text{Mg}^{2+}}$ and β_d (Figure 6b), $\alpha_{\text{Mg}^{2+}}$ is relatively low in zone I, where it is generally less than 6 mmol/L and locally less than 4 mmol/L, and is mainly distributed to the east of Rongcheng County. $\alpha_{\text{Mg}^{2+}}$ is relatively high in zone I₂ and higher than 6 mmol/L in some areas. β_d gradually increases along with the groundwater flow direction; it is generally less than two in zone I and greater than two in zone II. The maximum value is 3.47, which occurs to the south of Baiyangdian Lake.

According to the isoline maps showing $a_{\text{SO}_4^{2-}}$ and β_g (Figure 6c), $a_{\text{SO}_4^{2-}}$ is less than 4 mmol/L in zone I and is more than 4 mmol/L in zone II; β_g in zone I is generally less than -2 , and is less than -1 in zone II; in the groundwater funnel in the east of Xiongqian County, $a_{\text{SO}_4^{2-}}$ and β_g increased with the groundwater flow direction.

According to Figure 6d, α_{Cl^-} is less than 4 mmol/L in zone I and more than 4 mmol/L in zone II. β_h is generally less than -6.5 in zone I and greater than 6.5 in zone II; the maximum value is -4.37 .

The chemical potential field (Figure 3) of groundwater is consistent with the characteristics of groundwater movement reflected by the seepage field of groundwater in this

area; thus, the activity and saturation index of the hydrochemical index increase gradually along the direction of groundwater flow (Figure 3 blue arrow). In the process of groundwater exploitation, a change of water level (head) will locally change the groundwater flow field and affect the hydrochemical index. Generally, the groundwater flow conditions in zone I are relatively smooth, and the water chemistry types are predominantly $\text{HCO}_3\text{-Ca}$ and $\text{HCO}_3\text{-Ca}\cdot\text{Mg}$. From the perspective of the groundwater flow path, there is a trend of groundwater flow from the surrounding area toward Baiyangdian Lake, along with increasing ionic concentration and saturation indices. The hydrochemistry gradually changes from HCO_3 to $\text{HCO}_3\bullet\text{SO}_4$ and $\text{HCO}_3\bullet\text{Cl}$ in zone II. After entering the lake, the hydrochemistry changes to $\text{SO}_4\text{-HCO}_3$. The hydrogeological parameters were calculated using the groundwater chemical kinetics method.

As the terrain of the study area is flat, the depth of shallow groundwater can represent the characteristics of groundwater flow in the interior of the study area. Through a correlation between the depth of shallow groundwater and each ion, the migration characteristics of water flow for each ion can be qualitatively described for any location [36]. This, combined with the geological, geomorphologic, hydrogeological and hydrochemical conditions, allowed us to divide the study area into two zones (I ($\beta_c > 1$) and II ($\beta_c < 1$, water level < -25 m)) and four subzones (I_1 , I_2 , II_1 and II_2) according to the mineral saturation index contours (Figure 3).

3.2. Calculation of Hydrogeological Parameters

According to the ionic activity of each component and the saturation index of each mineral (Figure 6), the hydraulic conductivity was obtained (based on field aquifer test results) and the reaction rate constant was calculated by selecting 16 groups of sampling points in the direction of groundwater flow. These 16 groups of sampling points basically covered four subzones, with a length of 5 to 10 km and no crossing. The groundwater chemical kinetics results are shown in Table 1.

Table 1. Chemical reaction rate constant for each zone of the study area.

Area Number	Reaction Rate Constant/ $(\times 10^{-8} \text{ mol}^{-1}\cdot\text{d}^{-1})$			
	k_c	k_d	k_g	k_h
zone I_1	0.845	0.299	0.063	0.008
zone I_2	9.031	0.145	0.372	0.086
zone II_1	1.199	0.030	0.063	0.008
zone II_2	23.971	0.720	4.011	0.259

The hydraulic conductivity was obtained for different positions of shallow groundwater. The hydraulic conductivity measurements at each sampling point in each zone are listed in Table 2, which reveals an average hydraulic conductivity of between 2.75 m/d and 7.29 m/d for the study area. The hydraulic conductivity value calculated by the groundwater chemical kinetic method was verified using aquifer test data, and the two results are compared in Table 3. The values derived using groundwater chemical kinetics are approximately consistent with those derived using the traditional hydrogeological calculation method (aquifer tests), but slightly lower. The reason for this difference is as follows. First, the hydrogeological parameters calculated by aquifer tests only represent the hydrogeological conditions around the pumping well, whereas the groundwater kinetic method reflects the changing seepage field and hydrochemical potential field [31]. Second, different geological conditions may affect the permeability values. The study area is located in an alluvial-diluvial and alluvial-lacustrine plain, where most of the aquifers exist in the form of paleo-channels, which are locally continuous, with different aquifer thicknesses, heterogeneity and non-isotropy. Thus, it is possible that the theoretical values calculated by aquifer tests and groundwater chemical kinetics are not universal. Despite the influence of these two effects, the calculation results are similar for both methods, indicating that the method of groundwater chemical kinetics can be used to obtain groundwater kinetic

parameters in areas with a dense distribution of wells via sampling and testing. This can compensate for a lack of aquifer test data in local areas, which can replenish the calculation of hydrogeological parameters.

Table 2. Hydraulic conductivity calculated at each sampling point in the study area.

Area Number	Potential Lines Number	Aquifer Test (<i>m/d</i>)	Hydraulic Conductivity (<i>m/d</i>)	Average Hydraulic Conductivity (<i>m/d</i>)
zone I ₁	1	6.43	5.51	5.66
	2	-	2.97	
	3	-	7.63	
	4	-	1.07	
	5	8.90	7.93	
	6	-	3.77	
	12	-	9.14	
	13	-	2.36	
	16	-	10.51	
zone I ₂	7	-	5.66	7.29
	8	-	8.92	
zone II ₁	9	-	3.68	2.75
	10	-	3.20	
	11	-	1.36	
zone II ₂	14	-	2.95	3.05
	15	-	3.16	

Table 3. Hydraulic conductivity calculated by the chemical kinetics method and the aquifer test (*m/d*).

Area Number	Chemical Kinetics Method	Aquifer Test
zone I ₁	5.66	6.49
zone I ₂	7.29	8.09
zone II ₁	2.75	2.8
zone II ₂	3.05	3.26

As shown in Table 4, the retention time of groundwater in zone I₁ and zone I₂ is relatively short (0.14–0.86 a), with average values of 0.48 a and 0.44 a, respectively, and the flow rate is relatively high. The actual average groundwater velocity in these zones is 16.78 *m/d* and 22.21 *m/d*, respectively. The groundwater retention time in zone II₁ is relatively long, with an average value of 2.62 a and an average velocity of 4.75 *m/d*. The average retention time in zone II₂ is shorter than that in zone II₁ (0.26 a), whereas the average velocity is higher (26.35 *m/d*).

Table 4. Groundwater storage time (a) and actual groundwater velocity (*m/d*) at each sampling point in the different zones of the study area.

Area Number	Potential Lines Number	Retention Time/(a)	Velocity/(<i>m/d</i>)
zone I ₁	1	0.53	15.98
	2	0.86	9.16
	3	0.17	23.27
	4	0.67	5.24
	5	0.14	29.02
	6	0.78	9.69
	12	0.58	18.58
	13	0.42	12.78
	16	0.17	27.28
	average		0.48

Table 4. Cont.

Area Number	Potential Lines Number	Retention Time/(a)	Velocity/(m/d)
zone I ₂	7	0.74	7.48
	8	0.14	36.94
	average	0.44	22.21
zone II ₁	9	0.54	8.16
	10	4.68	2.58
	11	2.64	2.97
	average	2.62	4.57
zone II ₂	14	0.24	24.70
	15	0.28	27.99
	average	0.26	26.35

3.3. Analysis of Groundwater Circulation Conditions

The study area belongs to the medium permeability zone ($1 \text{ m/d} < K \leq 10 \text{ m/d}$), as shown by the slightly higher hydraulic conductivity of zone I and zone II. These two zones are alluvial-proluvial and alluvial-lacustrine, which are closer to the upper reaches of the flow field. Zone II₁, the alluvial-lacustrine layer, has a lower hydraulic conductivity. Theoretically, the groundwater flow conditions are weak, and the water circulation conditions are not smooth. According to section H–H' (Figure 5), the aquifer in zone I is more continuous than that in zone II₁. Moreover, borehole data reveal that the aquifer lithology in zone I and zone II₂ is coarser than that in zone II₁. Therefore, the hydrogeology, hydrogeochemistry, and groundwater chemical kinetics indicate that alluvial, alluvial-alluvial and alluvial-lacustrine strata influence the circulation of groundwater in terms of structure and permeability.

A quantitative evaluation of the changes in groundwater characteristics can also be used to analyze the groundwater circulation conditions, which requires quantification of the actual velocity and retention time of groundwater. According to previous research [37], water circulation can be completed in an aquifer in hydrogeological units with fast water circulation and a groundwater velocity of $\geq 1 \text{ m/d}$ after $t \leq 10 \text{ a}$. The shallow groundwater cycle in Xiong'an New Area is characterized as an alternating fast zone. In zone II₁, located in and around Baiyangdian Lake, the aquifer is characterized by relatively fine particles, a lack of development, poor hydraulic connection and relatively slow water cycle changes. The average groundwater flow velocity in this zone is 72–79% slower than that in zone I, and the average retention time is 4.5–5 times longer than that in zone I. Zone II₂, located in the drawdown funnel area, exhibits increased groundwater flow velocity because of the large artificial mining area within the scope of the hydraulic gradient. Specifically, the average groundwater flow is 19–57% faster than that in zone I and the average retention time is 42–47% shorter than that in zone I. This indicates that groundwater characteristics are affected not only by the hydrogeological structure, but also by over-exploitation, which will affect the actual velocity, retention time and circulation conditions of groundwater, as revealed by hydrogeochemical and groundwater chemical kinetics parameters.

3.4. Revealing the Burial Conditions of Paleo-Channels by Groundwater Chemical Kinetics

Large scale drilling has been carried out in Xiong'an New Area. In the area with dense boreholes, the distribution of paleo-channels can be described by using borehole data and geomorphic data. Taking the west side of zone I₁ as an example, the density of boreholes can reach one borehole per square kilometer (Figure 7), and the extension of paleo-channels can be better described. Comparing the results of groundwater chemical kinetics calculations with the Middle Pleistocene paleo-channels, it can be observed that the path along the paleo-channel facilitates good connectivity within the aquifer, and the hydraulic conductivity is still relatively high, such as potential lines 1 and 5. If the path crosscuts a single paleo-channel, the result is still high, such as potential lines 3. However, if the path crosscuts multiple paleo-channels, for aquicludes or less permeable strata, as

shows on the Figure 7, hydraulic conductivity is small, such as potential lines 2 and 4. The difference in hydraulic conductivity in different directions with relation to the paleo-channel reflects the heterogeneity of aquifer parameters. This can also be explained in Zone II. The potential lines 14 and 15 do not trend along the paleo-channel and so the hydraulic conductivity calculated is much lower. In short, the permeability calculated by this method can be mutually confirmed against the distribution of the paleo-channels.

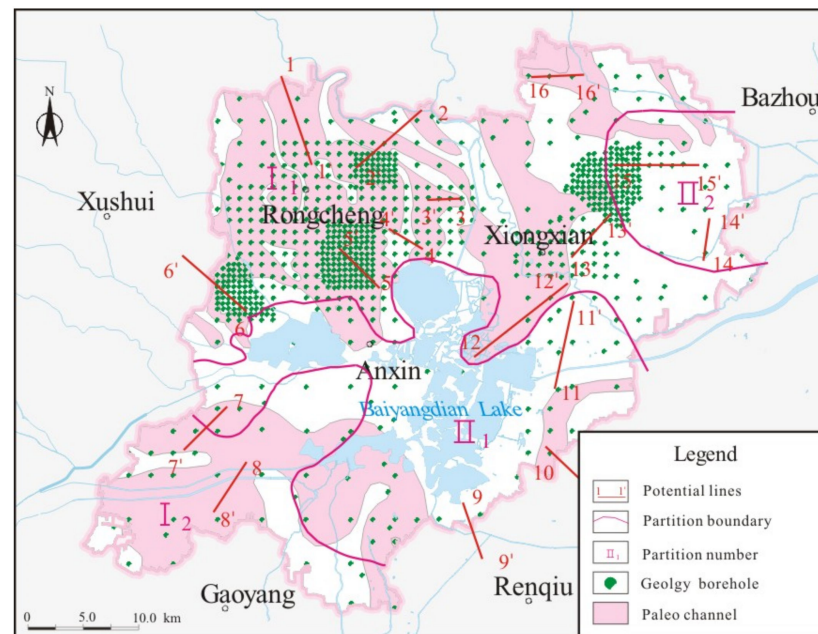


Figure 7. Modified paleo-channel distribution map in Qp^2 based on the results of boreholes and chemical kinetics.

This method has a certain control effect on areas with low borehole density. Taking potential line 12 as an example, the borehole density on the west side is low, and the borehole data cannot determine whether the paleo-channel extends to this location. The calculation results show that the hydraulic conductivity is 9.14 m/d . Compared with the calculation results in this area, it can be inferred that the area through which the potential line passes is within the paleo-channel course. The calculated hydraulic conductivity of potential lines 11 and 13 to the south is 1.36 m/d and 2.36 m/d . Combined with the stratigraphic information revealed by the borehole, it is inferred that the two potential lines are not within the scope of the paleo-channel. Using the information of potential lines 7 and 8, we can further infer the distribution of paleo-channels in area I_2 . The groundwater chemical kinetic method has certain advantages in the study of the unconsolidated groundwater aquifer in the paleo-channel.

4. Conclusions

Through the construction of a groundwater chemical kinetics model of alluvial-proluvial and alluvial-lacustrine groundwater aquifers in Xiong'an New Area, and the verification of hydrogeological parameters obtained by traditional hydrogeological survey methods, the important parameters of groundwater circulation can be obtained in detail, and the method is shown to be effective. This method partly addresses the lack of research into groundwater circulation of unconsolidated sedimentary aquifers dominated by paleo-channels. The main conclusions are as follows:

(1) The study area was divided into two zones and four subzones. The groundwater chemical kinetics parameters of shallow groundwater were calculated for each zone, and the chemical potential field of groundwater was determined according to major mineral saturation indices and ionic activity. The chemical potential field of groundwater was

consistent with the groundwater movement characteristics reflected by the groundwater seepage field.

(2) The groundwater chemical kinetics results of hydraulic conductivity along the paleo-channel are approximately consistent with traditional hydrogeological calculation results derived from aquifer test data. However, the scale effect and complex geological conditions of the study area resulted in the calculated hydraulic conductivity being slightly lower than that derived from field aquifer tests. The calculation method of groundwater chemical kinetics can compensate for a lack of aquifer test data in local areas, and can therefore help determine the hydrogeological parameters.

(3) A groundwater chemical kinetics model was established to evaluate the groundwater circulation conditions in Xiong'an New Area. Differences in hydrogeological parameters and changes in groundwater characteristics both affect the groundwater circulation conditions. Specifically, the difference in structure and permeability between alluvial-alluvial strata and alluvial-lacustrine strata affects the circulation of groundwater. Excessive groundwater exploitation will change the actual velocity and retention time of groundwater, which will influence the groundwater circulation conditions. Characterization of groundwater circulation in the study area was effectively achieved using the method of groundwater chemical kinetics.

(4) In the area with dense borehole concentration, the distribution of paleo-channels can be described by using borehole data and geomorphic data. Comparing the results of the groundwater chemical kinetics calculation with the distribution of the Middle Pleistocene paleo-channels, the data can be mutually confirmed. The difference in hydraulic conductivity in different directions with relation to the paleo-channel reflects the heterogeneity of aquifer parameters. This method has a certain control effect on areas with low borehole density, enabling the distribution of the paleo-channels to be inferred. The groundwater chemical kinetic method has certain advantages in the study of the unconsolidated groundwater aquifer within the paleo-channel.

Author Contributions: Conceptualization, Y.X. and H.L.; methodology, Y.X. and B.W.; investigation, C.Z., X.G. and K.Z.; data curation, Y.X. writing—original draft preparation, Y.X.; writing—review and editing, B.W. and Z.M.; supervision, Z.M.; project administration, Z.M.; resources, Y.X., H.L., Z.M., K.Z., X.G. and C.Z.; All authors have read and agreed to the published version of the manuscript.

Funding: This research was funded by China Geological Survey, grant numbers DD20189122, DD20189142, DD20190338 and DD20221759.

Institutional Review Board Statement: Not applicable.

Informed Consent Statement: Not applicable.

Data Availability Statement: Data sharing is not applicable.

Conflicts of Interest: The authors declare no conflict of interest.

References

1. Mattos, J.B.; Cruz, M.; Jeronimo, M.; Paula, F.D.; Carlos, F.; Sales, E.F. Spatio-seasonal changes in the hydrogeochemistry of groundwaters in a highland tropical zone. *J. S. Am. Earth Sci.* **2018**, *88*, 275–286. [[CrossRef](#)]
2. Redwan, M.; Moneim, A.A.A. Factors controlling groundwater hydrogeochemistry in the area west of Tahta, Sohag Upper Egypt. *J. Afr. Earth Sci.* **2016**, *118*, 328–338. [[CrossRef](#)]
3. Gupta, R.; Misra, A.K. Groundwater quality analysis of quaternary aquifers in Jhajjar District, Haryana, India: Focus on groundwater fluoride and health implications. *Alex. Eng. J.* **2016**, *57*, 375–381. [[CrossRef](#)]
4. Wang, D.C.; Zhang, R.Q. *General Hydrogeology*, 3rd ed.; Geological Publishing House: Beijing, China, 1986.
5. Cao, Y.Q.; Hu, K.R. *Groundwater Chemical Kinetics and Eco Environmental Zonation*, 1st ed.; Science Press: Beijing, China, 2009; pp. 5–8.
6. Liu, X.; Xiang, W.; Si, B.C. Hydrochemical and isotopic characteristics in the shallow groundwater of the Fenhe River basin and indicative significance. *Environ. Sci.* **2021**, *42*, 1739–1749. (In Chinese) [[CrossRef](#)]
7. Moral, F.; Cruz-Sanjulián, J.J.; Olías, M. Geochemical evolution of groundwater in the carbonate aquifers of sierra de segura (betic cordillera, southern Spain). *J. Hydrol.* **2008**, *360*, 281–296. [[CrossRef](#)]

8. Scheiber, L.; Cendón, D.I.; Iverach, C.P.; Hankin, S.I.; Vázquez-Suñé, E.; Kelly, B.F.J. Hydrochemical apportioning of irrigation groundwater sources in an alluvial aquifer. *Sci. Total Environ.* **2020**, *744*, 140506. [[CrossRef](#)] [[PubMed](#)]
9. Owen, D.D.R.; Cox, M.E. Hydrochemical evolution within a large alluvial groundwater resource overlying a shallow coal seam gas reservoir. *Sci. Total Environ.* **2015**, *523*, 233–252. [[CrossRef](#)] [[PubMed](#)]
10. Owen, D.D.R.; Pawlowsky-Glahn, V.; Egozcue, J.J.; Buccianti, A.; Bradd, J.M. Compositional data analysis as a robust tool to delineate hydrochemical facies within and between gas-bearing aquifers. *Water Resour. Res.* **2016**, *52*, 5771–5793. [[CrossRef](#)]
11. Guo, H.P.; Bai, J.B.; Zhang, Y.Q.; Wang, L.Y.; Shi, J.S.; Li, W.P.; Zhang, Z.C.; Wang, Y.L.; Zhu, J.Y.; Wang, H.G. The evolution characteristics and mechanism of the land subsidence in typical areas of the North China Plain. *Geol. China* **2017**, *44*, 1115–1127. (In Chinese) [[CrossRef](#)]
12. Siebert, S.; Henrich, V.; Frenken, K.; Burke, J. *Update of the Digital Global Map of Irrigation Areas to Version 5*; Food and Agriculture Organization of the United Nations: Rome, Italy, 2013. [[CrossRef](#)]
13. Sun, X.M.; Wu, D.D.; Xiao, G.Q.; Ma, Z.; Wang, W.D.; Xu, J.G.; Wang, L.H.; Xing, Z.X. Discussion on ground water research and geo-environment research in Circum-Bohai-Sea Region. *China. Geol. Surv. Res.* **2006**, *29*, 47–56.
14. Yan, J.H.; Chen, J.S.; Zhang, W.Q. Study on the groundwater quality and its influencing factor in Songyuan City, Northeast China, using integrated hydrogeochemical method. *Sci. Total. Environ.* **2021**, *773*, 144958. [[CrossRef](#)]
15. Zhao, K.; Qi, J.X.; Yi, C.; Ma, B.H.; Li, Y.; Guo, H.M.; Wang, X.Z.; Wang, L.Y.; Li, H.T. Hydrogeochemical characteristics of groundwater and pore-water and the paleoenvironmental evolution in the past 3.10 Ma in the Xiong'an New Area, North China. *China Geol.* **2021**, *4*, 476–486. [[CrossRef](#)]
16. Lu, B.Q.; Zhang, Y.; Sun, H.G.; Zheng, C.M. Lagrangian simulation of multi-step and rate-limited chemical reactions in multi-dimensional porous media. *Water Sci. Eng.* **2018**, *11*, 101–113. [[CrossRef](#)]
17. Peyraube, N.; Lastennet, R.; Denis, A. Geochemical evolution of groundwater in the unsaturated zone of a karstic massif, using the PCO₂–Slc relationship. *J. Hydrol.* **2012**, *430–431*, 13–24. [[CrossRef](#)]
18. Li, S.L.; Liu, C.Q.; Li, J.; Lang, Y.C.; Ding, H.; Li, L.B. Geochemistry of dissolved inorganic carbon and carbonate weathering in a small typical karstic catchment of Southwest China: Isotopic and chemical constraints. *Chem. Geol.* **2010**, *277*, 301–309. [[CrossRef](#)]
19. Hunkeler, D.; Mudry, J. Hydrochemical methods. In *Methods in Karst Hydrogeology*; IAH International Contributions to Hydrogeology; Goldscheider, N., Drew, D., Eds.; British Geological Survey: Wallingford, UK; Taylor & Francis Group e-Library: London, UK, 2007; pp. 93–121.
20. Mercado, A.; Billings, G.K. The kinetics of mineral dissolution in carbonate aquifers as a tool for hydrological investigations, i. concentration-time relationships. *J. Hydrol.* **1975**, *24*, 303–331. [[CrossRef](#)]
21. Dreybrodt, G.W. The impact of hydrochemical boundary conditions on the evolution of limestone karst aquifers. *J. Hydrol.* **2003**, *276*, 240–253. [[CrossRef](#)]
22. Ptak, T.; Schmid, G. Dual-tracer transport experiments in a physically and chemically heterogeneous porous aquifer: Effective transport parameters and spatial variability. *J. Hydrol.* **1996**, *183*, 117–138. [[CrossRef](#)]
23. Atchley, A.L.; Navarre-Sitchler, A.K.; Maxwell, R.M. The effects of physical and geochemical heterogeneities on hydro-geochemical transport and effective reaction rates. *J. Contam. Hydrol.* **2014**, *165*, 53–64. [[CrossRef](#)]
24. Guo, S.J.; Yu, L.; Ren, Z.W.; Wang, C.H.; Ming, Y.Y. Application of high-density resistivity method in fine division of Quaternary geological structure in the starting area of Xiongan New Area. *N. China Geol.* **2021**, *44*, 45–51. [[CrossRef](#)]
25. Liu, K.M.; Xu, Q.M.; Duan, L.F.; Niu, W.C.; Teng, F.; Wang, X.D.; Zhang, W.; Dong, J. Quaternary stratigraphic architecture and sedimentary evolution from borehole GB014 in the western Xiong'an New Area. *Sci. China Press* **2020**, *65*, 2145–2160. [[CrossRef](#)]
26. Wang, S.; Shao, J.; Song, X.; Zhang, Y.; Huo, Z.; Zhou, X. Application of MODFLOW and geographic information system to groundwater flow simulation in North China Plain. *China Environ. Geol.* **2008**, *55*, 1449–1462. [[CrossRef](#)]
27. Wang, Y.S.; Yin, D.C.; Qi, X.F.; Xu, R.Z. Hydrogen and Oxygen Isotopic Characteristics of Different Water and Indicative Significance in Baiyangdian Lake. *Environ. Sci.* **2021**, *43*, 1920–1929. [[CrossRef](#)]
28. Wang, Y.S.; Yin, D.C.; Wang, X.Q.; Qi, X.F.; Xia, Y.B.; Ma, Z.T.; Zhang, L.; Xu, R.Z. Groundwater- surface water interactions in the Baiyangdian wetland, Xiong'an New Area and its impact on reed land. *Geol. China* **2021**, *48*, 1368–1381.
29. Cao, Y.Q.; Hu, K.R. *Karst Hydrogeological Chemistry Environment*, 1st ed.; Jilin University Press: Changchun, China, 1994; pp. 13–34.
30. Geng, X.X.; Wang, F.G.; Gao, Z.K.; Cai, Z.M.; Gao, D.Y. Simulation of hydrochemical evolution characteristics in Yellow river irrigation area of Ling-Wu county. *Water. Sav. Iron.* **2013**, *2*, 29–33. (In Chinese)
31. Wang, N.; Cao, J.F.; Jiang, J.X.; Ping, J.H.; Shen, Y.Y.; Qin, L.J. Attempt to use the theory of hydrochemical dynamics to calculate the permeability coefficient of panshi's groundwater system. *J. Jilin Univ.* **2004**, *B10*, 74–79. (In Chinese) [[CrossRef](#)]
32. Sun, Y.Q.; Qian, H.; Duan, L. Impact of pH dissolution and precipitation of mineral in mixing solution. *J. Earth Sci. Environ.* **2009**, *31*, 413–417. [[CrossRef](#)]
33. Pokrovsky, O.S.; Golubev, S.V.; Schott, J. Dissolution kinetics of calcite, dolomite and magnesite at 25 °C and 0 to 50 atm pCO₂. *Chem. Geol.* **2005**, *217*, 239–255. [[CrossRef](#)]
34. Mayo, A.L.; Loucks, M.D. Solute and isotopic geochemistry and ground water flow in the central Wasatch Range, Utah. *J. Hydrol.* **1995**, *172*, 31–59. [[CrossRef](#)]
35. Chao, Y.Q.; Hu, K.R.; Hu, Z.Y. Hydrogeochemical reaction–migration—differentiation model. *J. Changchun Univ. Sci. Tech.* **2000**, *30*, 251–256. [[CrossRef](#)]

36. Liu, Y.; Lu, C.M.; Ma, R. Discriminant analysis on iron ion provenance in groundwater, eastern Hebei Plain. *Geol. Surv. Res.* **2019**, *42*, 135–142.
37. Kenoyer, G.J.; Bowser, C.J. Groundwater chemical evolution in a sandy silicate aquifer in northern Wisconsin: 1. Patterns and rates of change. *Water Resour. Res.* **1992**, *28*, 579–589. [[CrossRef](#)]